

STATE SPACE SYSTEM IDENTIFICATION AND IMPACT AIDED DAMPING RATIO ESTIMATION FOR A STRENGTHENED STONE MASONRY BUILDING

DIPENDRA GAUTAM^{*}, RABINDRA ADHIKARI[†], SIMON OLAFSSON^{*} AND
RAJESH RUPAKHETY^{*}

^{*} Earthquake Engineering Research Center, Faculty of Civil and Environmental Engineering
University of Iceland
Austurvegur 2a, 800 Selfoss, Iceland
e-mail: dig17@hi.is

[†] Department of Civil Engineering
Cosmos College of Management and Technology
Lalitpur, Nepal

Key words: System Identification, Free Vibration Response, Impact Excitation, Stone Masonry, Seismic Strengthening, Modal Frequency, Damping Ratio.

Summary. Through the formulation of a mathematical model from time series records, the poles and zeros can be evaluated for a dynamic system. This paper identifies the dynamic characteristics of a strengthened stone masonry prototype building using the splint-and-band technique. A two storied stone masonry building left after a demonstration test was subject to a series of impact excitations in the impact testing facility (shock table) and time series records were taken using three triaxial accelerometers. A series of impacts were deployed, and the vibration frequencies were estimated using the state space system identification technique implemented through the Numerical Algorithms for Subspace State Space System Identification (N4SID) method. After observing a significant damage aggravation, the vibration frequency along the longer wall direction was reduced to 3.38 Hz from 7.42 Hz, whereas the frequency along the short wall direction was reduced to 4.62 Hz from 5.82 Hz. The reduction in the vibration frequencies is attributed to damage induced by the impact loading. Since ambient vibration cannot excite the higher modes in a structure, blind system identification is often challenging. A further challenge arises while estimating the damping ratio since a free vibration response of a structure cannot be achieved through ambient vibration measurements. To overcome this challenge, a series of impacts were imposed, and the damping ratio was estimated using the free vibration response of the building. The damping ratio for the tested building is found to be 1.1%. Numerical analyses often use a higher value of damping ratio than the one estimated from the free vibration response. Since there is no unanimous agreement regarding the damping characteristics of stone masonry constructions, the results reported in this study could provide a rational basis for numerical modeling. This paper also presents sequential frequency reduction adhering to each impact. Some remarks on future instrumentation and output-only system identification are also provided.

1 INTRODUCTION

Structural system identification is a nondestructive dynamic characterization technique that uses some nonparametric or parametric formulations to obtain dynamic properties such as modal frequencies, modal damping ratios, and mode shapes. A key application of structural system identification is in modal tracking because fluctuations in the modal properties are fundamentally attributed to the changes in stiffness characteristics of the structures. Thus, damage detection [1, 2, 3], damage aggravation [4], changes in stiffness characteristics after strengthening [5], etc. can be characterized using nondestructive structural system identification. However, the primary application of system identification remains in the identification of modal characteristics that are used for structural engineering and geotechnical engineering applications [6, 7, 8, 9, 10, 11, 12, 13, 14, 15]. With the advancement of sensors and signal processing techniques, modal identification has gained considerable momentum in the past few decades. Many building typologies including reinforced concrete buildings and bridges, steel buildings and bridges, and brick and block masonry constructions, wooden buildings, among others have been extensively studied to date [1, 5, 10, 11, 14, 16, 17, 18, 19, 20]. On the contrary, stone masonry buildings have seldom been considered for operational modal analysis.

Across the Hindu Kush Himalaya and Karakoram as well as many other active seismic regions of the world, stone masonry is widely used as the principal construction system due to the immediate availability of resources. However, seismic performance of stone masonry is often questioned as reflected by its performance during historical earthquakes [21, 22, 23, 24, 25, 26]. Although high seismic vulnerability is well understood and accepted, numerical modeling is still challenging due to widespread uncertainties in stone masonry construction, ranging from material uncertainties, boundary conditions, and nonlinear response. Similarly, seismic strengthening of stone masonry construction has not gotten as much attention as reinforced concrete and brick masonry systems. Dynamic characteristics of strengthened stone masonry constructions are not well reported either. Since life safety is a very challenging issue for stone masonry and is often marred by the ad-hoc out of plane collapse of single or multiple wythes, rudimentary strengthening could be instrumental in saving lives during destructive earthquakes. For this, a general understanding of the dynamic characteristics of stone masonry is a pre-requisite. This paper reports the dynamic characteristics of a strengthened stone masonry in mud mortar building before and after impact aided damage aggravation. Frequencies and damping ratios of the test specimen are reported together with the insights from impact loading assisted system identification.

2 MATERIALS AND METHODS

2.1 Vibration testing

We performed vibration testing in a specimen prepared for demonstration purposes at the Institute of Engineering, Pulchowk Campus, Lalitpur, Nepal. All vibration tests reported in this paper are conducted after the demonstration. Thus, the dynamic characteristics reported in the paper are those of the model that has already undergone several cycles of impacts. The specimen was single story plus attic stone masonry in mud mortar construction prepared tentatively in a 1:2 scale. The dimensions of the specimen were 2.22×3.25×2.1 m. The specimen had four

openings resembling windows in the long wall direction and two openings in the short wall direction. We deployed three triaxial ETNA-2 accelerometers manufactured by Kinematics Inc., California. Time synchronization was done using externally connected GPS antennas. Vibration records were taken with several gentle impact blows and a few strong blows to induce damage to the structure. Vibration records were taken for 30 minutes under each impact at the sampling frequency of 100 Hz. Figure 1 shows an example of accelerometer setup for vibration recording. Although mounted on the table, one of the accelerometers drifted remarkably, and hence input-output system identification was not possible. Figure 2 shows the impact testing setup together with the impact hammer and table platform. The larger opening side is also shown in Figure 2. Seismic strengthening is provided in the model by deploying wire meshes and occasional ties to connect interior and exterior meshes.



Figure 1: Instrumentation for vibration recording.



Figure 2: Test setup showing impact hammer (right) and strengthened model.

Figure 3 shows a typical time series record obtained during impact testing. The figure highlights that the impact induced peak output acceleration reached up to 0.9g, where g is the acceleration of gravity. Minor drifts can be also observed in the time series. Whereas the

acceleration drops sharply immediately after releasing the impact.

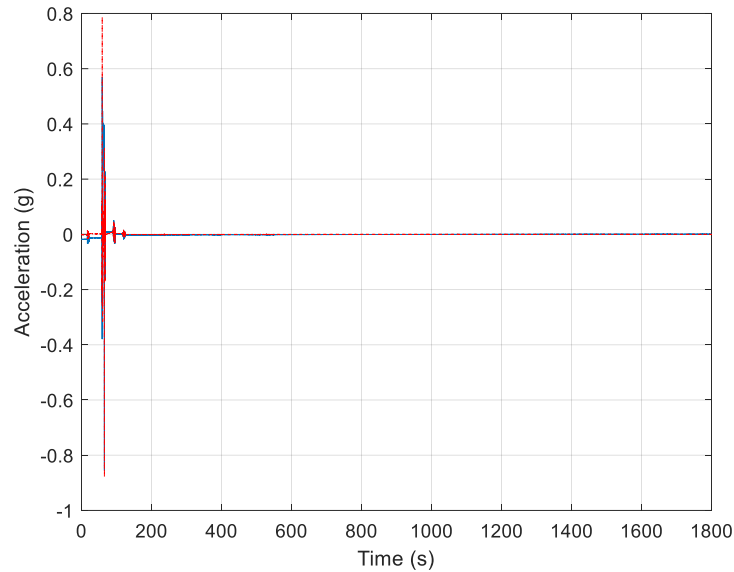


Figure 3: Output time series recorded during impact testing.

2.2 System identification

State space system identification is conducted to estimate vibration frequencies and damping ratios. In order to perform state space system identification, numerical algorithms for subspace state space system identification (N4SID) [27]. N4SID is a noniterative algorithm that does not require nonlinear optimization and extra parameterization in the initial state. Despite its commendable performance, N4SID does not require a priori knowledge of system order and controllability index either. The only input variable is the model order, which could be selected using a stabilization diagram. N4SID conducts oblique projection of subspaces acquired from the block Hankel matrix and provides dynamic characteristics using state matrices. Before deploying the system identification algorithm, time series data were transient corrected and tapered using the Tukey window. A fourth order Butterworth filter with 20 Hz corner frequency was used. System identification was conducted for two states, before and after impact aided damage occurrence. After the impact blow, some slices of free vibration records were also captured, and the damping ratio was estimated using the logarithmic decrement method. Further details regarding the logarithmic decrement method can be found in [28]. For the sake of brevity, mathematical details are not included in this paper.

3 RESULTS AND DISCUSSIONS

We performed parametric system identification using N4SID. Before deploying parametric system identification, Welch power spectral densities (PSD) were also plotted for the time series. Welch PSD is a nonparametric system identification approach in which peak picking can be performed to estimate tentative modal frequency. An example of transient and spike

corrected time series for all three axes is shown in Figure 4. Transient correction is done manually which requires meticulous judgment and decision making to obtain reliable time series.

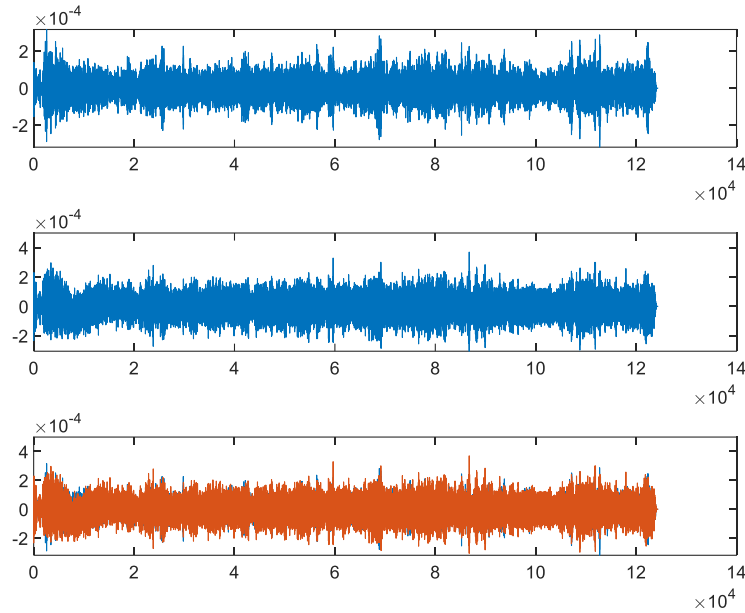


Figure 4: Transient and spike corrected time series.

Figure 5 shows the Welch PSD plots for the three time series records shown in Figure 4. The PSD plots for two horizontal components reflect at least three modal frequencies. Furthermore, the PSD plots indicate that the fundamental vibration mode is along the short wall direction of the building. From the peak, the fundamental frequency of the building can be estimated to be ~ 5.9 Hz.

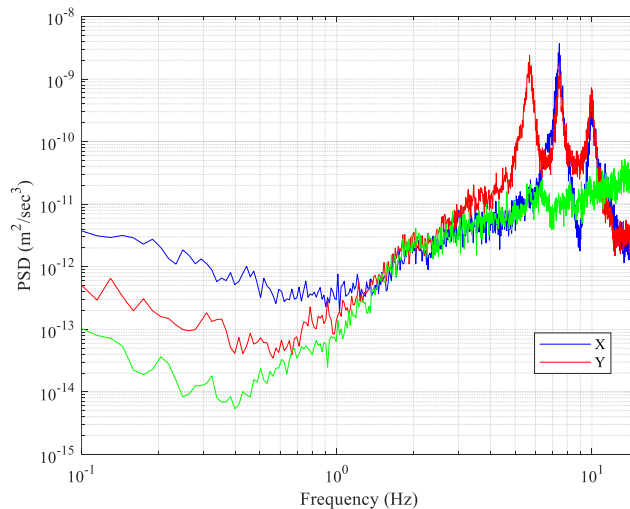


Figure 5: Welch PSD plots for two horizontal axes (X and Y) and a vertical (green) time series.

The frequency response function (FRF) plots for the two orthogonal time series records are presented in Figure 6. Akin to the PSDs, FRFs show three distinct peaks adhering to the first three modes of vibration along the two orthogonal directions. System characteristics are not extracted for the vertical direction since the impact cannot excite vertical direction and the vertical mode of vibration is not expected in early modes as opposed to the horizontal ones. Reliable vertical mode of vibration requires vertical excitation as well.

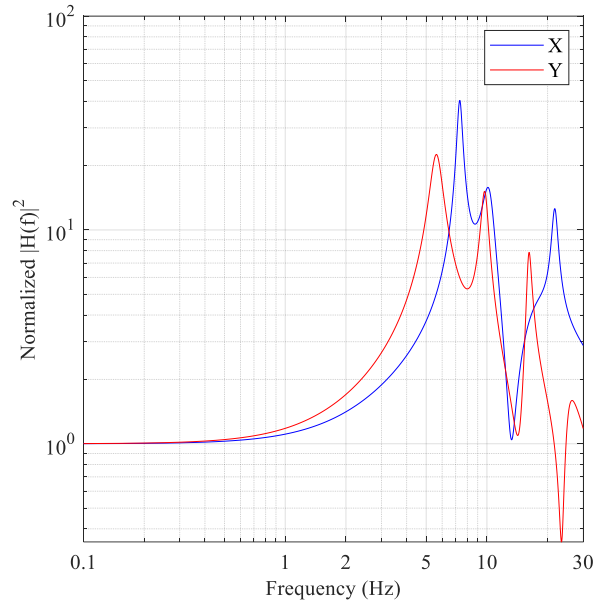


Figure 6: FRFs for two orthogonal directions of time series.

We performed system identification choosing a model order of 12. To select this value, the stabilization diagram was plotted first. An example of stabilization plot indicating the efficacy of model order 12 is shown in Figure 7.

System identification was performed twice before inducing impact aided damage to the structure. For the two sets of minor impact blows without damage, the system characteristics are summarized in Table 1. In the case of damage nonoccurrence, relatively similar modal characteristics are obtained from parametric system identification. The discrepancies between the two setups are attributed to the transient correction process since there is no stopping criteria to obtain comparable time series. In this case, some time series can have more transients than others and slight discrepancies may arise in system characteristics. If multiple records are available, then it is advisable to perform averaging between the setups to obtain final dynamic characteristics. It is also worth mentioning that the windowing is done to divide the whole 30-minute time series into five segments and the obtained dynamic characteristics are the average values from the five windows. This two-layer averaging is efficient in enhancing the reliability of the estimated parameters. From the free vibration time series segment, the damping ratio (ζ) is estimated to be 1.10%, which is lower than the N4SID value.

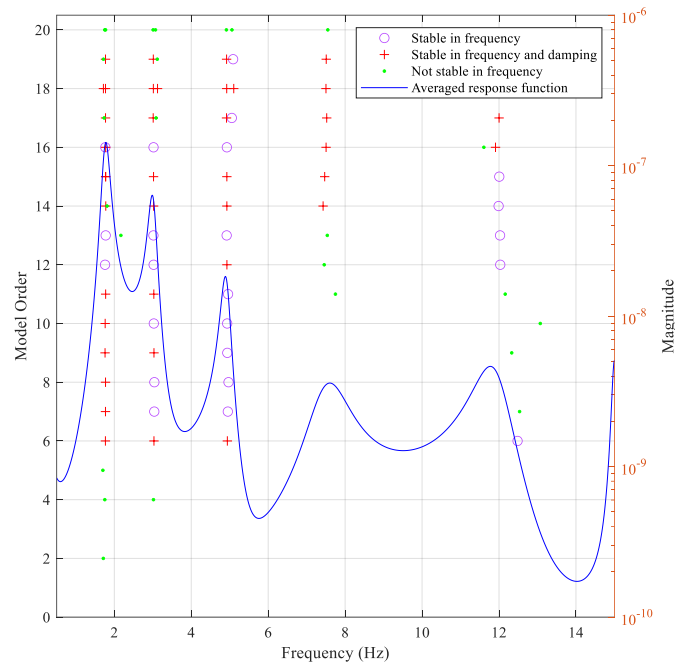


Figure 6: Stabilization diagram indicating the efficacy of particular model order.

Table 1: Dynamic characteristics of the specimen before impact aided damage.

Mode	Setup I			Setup II		
	f_x (Hz)	f_y (Hz)	ζ (%)	f_x (Hz)	f_y (Hz)	ζ (%)
I	7.42	5.82	1.58	7.36	5.90	1.36
II	10.06	9.81		10.12	9.46	
III	21.10	19.55		15.22	15.18	

Several impact blows were deployed to the table and damage was induced to the specimen. Damage to the structural wall was observed in several locations as shown in Figure 7. Similarly, wire meshes were broken in several locations, which confirms the damage occurrence and stiffness reduction. The FRF after damage is shown in Figure 8. The figure shows a shift in the fundamental vibration direction together with a significant reduction in the frequency. The summary of vibration characteristics after damage is presented in Table 2. The damping ratio is found to be increased significantly after damage. A considerable reduction along the longer wall side is attributed to the greater intensity of the damage. A 54.45% reduction in frequency is envisaged after the impact aided damage. However, we were not able to quantify the force application so as to quantify the level of frequency reduction given the impact loading. On the other hand, the Y direction observed only a 20.62% reduction in the first mode frequency, which is attributed to lesser damage to the short wall direction. We have reported the first three vibration mode results only because higher modes except for the first three are not reliably estimated as shown in Figure 6.



Figure 7: Impact aided damage to the specimen.

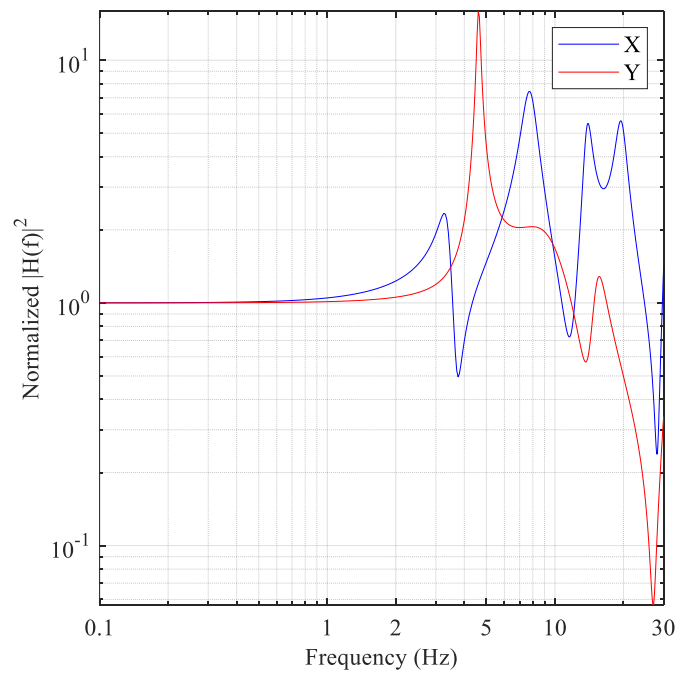


Figure 8: FRF for the damaged state time series records.

Table 2: Dynamic characteristics of the specimen after impact aided damage.

Mode	f_x (Hz)	f_y (Hz)	ζ (%)
I	3.38	4.62	1.95
II	7.76	9.45	
III	13.85	15.35	

4 CONCLUSIONS

In an attempt to quantify the effect of dynamic characteristics (frequencies and damping ratio) of strengthened stone masonry in mud mortar specimen using rudimentary seismic enhancement, we performed system identification before and after impact aided damage. The significant reduction in the frequency characteristics is found to be well attributed to the structural damage. This undergirds the use of periodic vibration time series recording and subsequent damage detection. We also characterized the damping ratio of the strengthened stone masonry and found it to be in the range of 1.38-1.58%. Whereas the logarithmic decrement method yielded a damping ratio of 1.10% only. This indicates that the damping ratio of stone masonry in mud mortar is lower than in other construction systems such as reinforced concrete structures. We conclude that the major issue in system identification is transient and spike handling as both affect the system characteristics significantly. In order to estimate reliable system characteristics, transient and spike correction, signal tapering, and appropriate filtration are required. Thereafter, state space system identification is found to yield reliable system parameters in before and after impact aided damage induction. Future studies can incorporate numerical model refinement using the vibration characteristics identified in this study.

7 ACKNOWLEDGMENTS

We thank Kshitij Charan Shrestha, Uddav Bhattarai, Lalit Bhatt, and Manish Man Shrestha for helping us to conduct the dynamic testing.

REFERENCES

- [1] Gautam, D., R. Adhikari, A. Niraula, S. Olafsson, and R. Rupakhety, "Dynamic identification and damage detection for a Greco-roman monument," in *Structural Analysis of Historical Constructions. SAHC 2023.*, vol. 47, Y. Endo and T. Hanazato, Eds., RILEM Bookseries, 2024, pp. 678–689.
- [2] Kuwabara, M., S. Yoshitomi, and I. Takewaki, "A new approach to system identification and damage detection of high-rise buildings," *Struct Control Health Monit*, vol. 20, no. 5, 2013, doi: 10.1002/stc.1486.

- [3] Gallipoli, M. R. *et al.*, “Structural health monitoring of the Ferrara University before and after the 2012 Emilia (Italy) earthquake, and after the damage repairs,” *Struct Health Monit*, vol. 19, no. 3, 2020, doi: 10.1177/1475921719866439.
- [4] Gautam, D., S. Olafsson, and R. Rupakhety, “System identification based structural damage aggravation detection in a large masonry building,” *Procedia Structural Integrity*, vol. 58, pp. 102–108, 2024, doi: 10.1016/j.prostr.2024.05.017.
- [5] Gautam, D., R. Adhikari, S. Olafsson, and R. Rupakhety, “Damage description, material characterization, retrofitting, and dynamic identification of a complex neoclassical monument affected by the 2015 Gorkha, Nepal earthquake,” *Journal of Building Engineering*, vol. 80, p. 108152, 2023, doi: 10.1016/j.job.2023.108152.
- [6] Foti, D., V. Gattulli, and F. Potenza, “Output-only identification and model updating by dynamic testing in unfavorable conditions of a seismically damaged building,” *Computer-Aided Civil and Infrastructure Engineering*, vol. 29, no. 9, 2014, doi: 10.1111/mice.12071.
- [7] Foti, D., N. I. Giannoccaro, V. Vacca, and M. Lerna, “Structural operativity evaluation of strategic buildings through finite element (Fe) models validated by operational modal analysis (oma),” *Sensors (Switzerland)*, vol. 20, no. 11, 2020, doi: 10.3390/s20113252.
- [8] Foti, D., M. Diaferio, N. I. Giannoccaro, and M. Mongelli, “Ambient vibration testing, dynamic identification and model updating of a historic tower,” *NDT and E International*, vol. 47, 2012, doi: 10.1016/j.ndteint.2011.11.009.
- [9] Gallipoli, M. R., T. A. Stabile, P. Guéguen, M. Mucciarelli, P. Comelli, and M. Bertoni, “Fundamental period elongation of a RC building during the Pollino seismic swarm sequence,” *Case Studies in Structural Engineering*, vol. 6, 2016, doi: 10.1016/j.csse.2016.05.005.
- [10] Gautam, D., R. Adhikari, S. Olafsson, and R. Rupakhety, “Dynamic identification of an aging prestressed concrete bridge using heavy vehicle excitation,” *Soil Dynamics and Earthquake Engineering*, vol. 173, p. 108127, Oct. 2023, doi: 10.1016/j.soildyn.2023.108127.
- [11] Dhakal, R., R. Rupakhety, and D. Gautam, “System Identification and Seismic Performance Assessment of Representative RC Buildings in Kathmandu Valley,” *Front Built Environ*, vol. 6, 2020, doi: 10.3389/fbuil.2020.601116.
- [12] Rupakhety, R., D. Gautam, R. Adhikari, P. Jha, L. Bhatt, and R. Baruwal, “System Identification and Finite Element Modelling of Damaged Bal Mandir Monument in Kathmandu After the 2015 Gorkha Earthquake,” 2022, pp. 222–231. doi: 10.1007/978-3-030-90788-4_21.

- [13] Sawaki, Y., R. Rupakhety, S. Ólafsson, and D. Gautam, *System identification of a residential building in Kathmandu using aftershocks of 2015 Gorkha earthquake and triggered noise data*, vol. 47. 2019. doi: 10.1007/978-3-319-78187-7_18.
- [14] Gautam, D., S. Olafsson, and R. Rupakhety, “Operational modal analysis of non-redundant wood frame building,” in *9th International Conference on Computational Methods in Structural Dynamics and Earthquake Engineering (COMPDYN 2023)*, M. Papadrakakis and M. Fragiadakis, Eds., Athens, Jun. 2023.
- [15] Bassoli, E., L. Vincenzi, A. M. D’Altri, S. de Miranda, M. Forghieri, and G. Castellazzi, “Ambient vibration-based finite element model updating of an earthquake-damaged masonry tower,” *Struct Control Health Monit*, vol. 25, no. 5, 2018, doi: 10.1002/stc.2150.
- [16] Vidal, F., M. Navarro, C. Aranda, and T. Enomoto, “Changes in dynamic characteristics of Lorca RC buildings from pre- and post-earthquake ambient vibration data,” *Bulletin of Earthquake Engineering*, vol. 12, no. 5, 2014, doi: 10.1007/s10518-013-9489-5.
- [17] Sivori, D., M. Lepidi, and S. Cattari, “Ambient vibration tools to validate the rigid diaphragm assumption in the seismic assessment of buildings,” *Earthq Eng Struct Dyn*, vol. 49, no. 2, 2020, doi: 10.1002/eqe.3235.
- [18] Di Cesare, A. *et al.*, “Identification of the structural model and analysis of the global seismic behaviour of a RC damaged building,” *Soil Dynamics and Earthquake Engineering*, vol. 65, 2014, doi: 10.1016/j.soildyn.2014.06.005.
- [19] Gallipoli, M. R. *et al.*, “Empirical estimates of dynamic parameters on a large set of European buildings,” *Bulletin of Earthquake Engineering*, vol. 8, no. 3, 2010, doi: 10.1007/s10518-009-9133-6.
- [20] Serlenga, V. *et al.*, “An integrated approach for structural behavior characterization of the Gravina Bridge (Matera, Southern Italy),” *Struct Health Monit*, vol. 20, no. 6, 2021, doi: 10.1177/1475921720987544.
- [21] Chettri, N., D. Gautam, and R. Rupakhety, “Seismic Vulnerability of Vernacular Residential Buildings in Bhutan,” *Journal of Earthquake Engineering*, 2021, doi: 10.1080/13632469.2020.1868362.
- [22] Gautam, D., N. Chettri, K. Tempa, H. Rodrigues, and R. Rupakhety, “Seismic vulnerability of Bhutanese vernacular stone masonry buildings: From damage observation to fragility analysis,” *Soil Dynamics and Earthquake Engineering*, 2022, 160:107351.

- [23] Gautam, D., “Observational fragility functions for residential stone masonry buildings in Nepal,” *Bulletin of Earthquake Engineering* 2018, vol. 16, no. 10, pp. 4661–4673, Apr. 2018, doi: 10.1007/S10518-018-0372-2.
- [24] Gautam, D., G. Fabbrocino, and F. Santucci de Magistris, “Derive empirical fragility functions for Nepali residential buildings,” *Eng Struct*, 2018, doi: 10.1016/j.engstruct.2018.06.018.
- [25] Ahmad, N., Q. Ali, M. Ashraf, B. Alam, and A. Naeem, “Seismic vulnerability of the Himalayan half-dressed rubble stone masonry structures, experimental and analytical studies,” *Natural Hazards and Earth System Sciences*, vol. 12, no. 11, 2012, doi: 10.5194/nhess-12-3441-2012.
- [26] Cuadra, C., “Dynamic characteristics of Inca’s stone masonry,” in *Masonry Construction in Active Seismic Regions*, 2021. doi: 10.1016/B978-0-12-821087-1.00002-8.
- [27] van Overschee, P., and B. de Moor, “N4SID: Subspace algorithms for the identification of combined deterministic-stochastic systems,” *Automatica*, vol. 30, no. 1, 1994, doi: 10.1016/0005-1098(94)90230-5.
- [28] Clough R. W. and J. Penzien, *Dynamics of Structures*. McGraw-Hill, 1975.